

Gerson H. Cohen,<sup>a\*</sup> Enid W. Silverton,<sup>a†</sup> Eduardo A. Padlan,<sup>a§</sup> Fred Dyda,<sup>a</sup> Jamie A. Wibbenmeyer,<sup>b</sup> Richard C. Willson<sup>b</sup> and David R. Davies<sup>a</sup>

<sup>a</sup>National Institutes of Health, 5 Center Drive, MSC 0560, Bethesda, MD 20892-0560, USA, and <sup>b</sup>Departments of Chemical Engineering and Biology and Chemistry, University of Houston, TX 77004-4004, USA

† Deceased.

§ Present address: Marine Science Institute, College of Science, University of the Philippines Diliman, Quezon City, Phillipines.

Correspondence e-mail: gerson.cohen@nih.gov

## Water molecules in the antibody–antigen interface of the structure of the Fab HyHEL-5–lysozyme complex at 1.7 Å resolution: comparison with results from isothermal titration calorimetry

The structure of the complex between hen egg-white lysozyme and the Fab HyHEL-5 at 2.7 Å resolution has previously been reported [Cohen *et al.* (1996), *Acta Cryst. D* **52**, 315–326]. With the availability of recombinant Fab, the X-ray structure of the complex has been re-evaluated at 1.7 Å resolution. The refined structure has yielded a detailed picture of the Fab–lysozyme interface, showing the high complementarity of the protein surfaces as well as several water molecules within the interface that complete the good fit. The model of the full complex has improved significantly, yielding an  $R_{\text{work}}$  of 19.5%. With this model, the structural results can be compared with the results of isothermal titration calorimetry. An attempt has been made to estimate the changes in bound waters that accompany complex formation and the difficulties inherent in using the crystal structures to provide the information necessary to make this calculation are discussed.

Received 9 February 2005

Accepted 11 March 2005

**PDB Reference:** HyHEL-5–lysozyme complex, 1yqv, r1yqvsf.

### 1. Introduction

Most protein molecules carry out their functions either in a permanent or temporary association with other proteins. These complexes range from simple homodimers to large arrays and their structures reveal the nature of the specificity of interaction and the forces involved in forming these associations. Antibody complexes with protein antigens, an essential part of the immune system, are being increasingly studied as examples of simple dimeric complexes. Since both antibodies and their protein antigens when uncomplexed are soluble proteins, their interacting surfaces are likely to be reasonably polar in character and, when isolated, would be in contact with a layer of bound water molecules. The analysis of several such complexes has demonstrated the relative contributions of shape complementarity, hydrogen bonding and the role of interfacial waters in determining the specificity of the antibody–antigen interaction (Bhat *et al.*, 1994; Braden *et al.*, 1994, 1998; Chacko *et al.*, 1995, 1996; Cohen *et al.*, 1996; Dall'Aqua *et al.*, 1998; Fields *et al.*, 1996; Kondo *et al.*, 1999; Lawrence & Colman, 1993; Malby *et al.*, 1994; Monaco-Malbet *et al.*, 2000; Mylvaganam *et al.*, 1998; Tulip *et al.*, 1992; Yili *et al.*, 2000, 2003).

The structure of the antibody–antigen complex of HyHEL-5 Fab with lysozyme has been investigated previously by X-ray crystallography (Cohen *et al.*, 1996) and by other experimental and computational studies (Xavier *et al.*, 1997; Xavier & Willson, 1998; Wibbenmeyer, Schuck *et al.*, 1999). The earlier X-ray studies of the complex were performed with Fab that was proteolytically derived from the intact antibody.

Here, we report a study of the HyHEL-5 complex with lysozyme using recombinant Fab for which the individual chains have been cloned and expressed in *Escherichia coli* (Wibbenmeyer, Xavier *et al.*, 1999). These crystals diffract significantly better than the original crystals, permitting a credible location of the water molecules in the interacting surfaces and providing a basis for estimating the change in bound waters when the two proteins interact. Contrary to naive expectation, several groups have reported an increase in the number of bound waters as a result of complex formation (Xavier *et al.*, 1997). In this report, we present crystallographic results regarding the number of waters involved in the antigen–antibody interface of the complex. We also discuss some of the potential pitfalls in estimating the change in the number of waters in this interface in comparison with the number of waters associated with the same surfaces of the uncomplexed antigen and antibody.

## 2. Methods

Recombinant HyHEL-5 Fab protein was prepared as described in Wibbenmeyer, Xavier *et al.* (1999). Crystals of the complex of the Fab with lysozyme were prepared as described previously for the proteolytically cleaved Fab (Sheriff, Silverton *et al.*, 1987). The crystals obtained are of the so-called ‘long-axis’ form found in previous work, with unit-cell parameters  $a = 54.46$ ,  $b = 74.26$ ,  $c = 78.26$  Å,  $\beta = 101.6^\circ$  and space group  $P2_1$ . Diffraction data to 1.7 Å were collected at 95 K on an R-AXIS I system. Data were processed with the *HKL* program suite (Otwinowski & Minor, 1997), yielding the statistics shown in Table 1.

The earlier model for the complex (PDB code 3hfl; Cohen *et al.*, 1996), with water molecules removed, served as the starting point of the refinement. Rigid-body refinement (*X-PLOR* v.3.1; Brünger, 1992) using 10.0–3.0 Å data with  $F_{\text{obs}} \geq 2.0\sigma(F)$  on the lysozyme, the Fv domain and the  $C_{\text{L}}:C_{\text{H1}}$  domain resulted in an  $R$  factor of 0.34. Alternating cycles of model building and structure refinement were performed, initially using data only to 2.5 Å, then gradually including more data until all reflections to 1.7 Å were used. Model building was accomplished using the program *O* (Jones *et al.*, 1991) with  $2F_o - F_c$  and  $F_o - F_c$  maps. Initial model refinement was performed with data having  $F_{\text{obs}} \geq 3.0\sigma(F)$ , with alternate simulated-annealing positional and thermal factor cycles and the parameter set of Eng & Huber (1991) in *X-PLOR*. A test set of 5% randomly chosen reflections was used for the calculation of  $R_{\text{free}}$  (Brünger, 1997). Solvent molecules were located automatically from  $F_o - F_c$  maps using *MAPMAN* (Kleywegt & Jones, 1996) at various stages of the refinement and confirmed with *X-PLOR* as well as by visual inspection. *CNS* v.1.0 (Brünger *et al.*, 1998) was subsequently employed using overall anisotropic temperature-factor correction, a bulk-solvent mask, maximum-likelihood target correction and all non-negative diffraction data. Final validation and location of water sites was carried out with *CNS*, using procedures provided in the program suite with standard parameters followed by visual inspection. Solvent molecules

**Table 1**

Summary of crystallographic data.

Values in parentheses refer to the highest resolution shell.

Space group	$P2_1$
Unit-cell parameters	$a = 54.46$ , $b = 74.26$ , $c = 78.26$ , $\alpha = 90$ , $\beta = 101.6$ , $\gamma = 90$
Oscillation data collected on 185 1.0° images at 95 K	
Wavelength (Å)	1.542 (Cu $K\alpha$ )
Resolution range (Å)	30–1.7 (1.74–1.7)
Observed reflections	117428 (3428)
Independent reflections	62951 (2767)
Completeness (%)	94 (58)
$I/\sigma(I)$	16.3 (1.9)
$R_{\text{sym}}$ (%)	5.5 (29.4)
Refinement using <i>CNS</i>	
Resolution range (Å)	30–1.7 (1.78–1.7)
Completeness	
Working set (%)	84 (53)
Free set (%)	4 (3)
$R_{\text{work}}$ (%)	19.5 (29.1)
$R_{\text{free}}$ (%)	23.4 (27.5)
No. of residues	555
No. of water molecules	619
Geometry: r.m.s. deviations	
Bond lengths (Å)	0.005
Bond angles (°)	1.29

with high thermal factors were individually examined and removed unless they appeared to be involved in reasonable contacts with protein. Candidate solvent molecules that were not reasonably near protein or that were not located in density in a  $2F_o - F_c$  map were also removed.

Molecular comparisons were carried out using *ALIGN* (Cohen, 1997). Surface calculations and the study of cavities and interfaces were made with the *MS* program suite (Connolly, 1983) and *CONTACSYM* (Sheriff, Hendrickson *et al.*, 1987) using a probe radius of 1.5 Å. Shape complementarity,  $S_c$ , a measure that approaches 1.0 when a pair of surfaces has a constant ‘ideal’ separation throughout with normals that are antiparallel, was calculated by the method of Lawrence & Colman (1993).

### 2.1. Model quality

Refinement statistics are shown in Table 1. The stereochemistry of this model is significantly better than that of the previous model. Only one non-glycine residue falls in a disallowed  $\varphi$ ,  $\psi$  region, Thr51<sub>L</sub>. The  $\varphi$ ,  $\psi$  angles for this residue of CDR L2 identify it as a class 3  $\gamma$ -turn (Milner-White & Poet, 1987), consistent with L2 of other Fab light chains (Milner-White *et al.*, 1988).

During refinement, a sequence error was discovered in the PDB models 2hfl and 3hfl. Two residues in positions 199–200 of  $C_{\text{H1}}$  that had initially been assigned as Pro-Arg were corrected to Thr-Trp, in agreement with the DNA sequence. This correction also improved the fit in the maps for 3hfl.

The cloned sequence (Wibbenmeyer, Xavier *et al.*, 1999) differs in several residues from the sequence of Kabat *et al.* (1987). In both the light and heavy chains a methionine has been inserted prior to the first residue; the next residue of  $V_{\text{H}}$  is Glu in place of pyroglutamate. The electron-density maps

reveal the methionine of the light chain but not of the heavy chain. At the end of  $C_{HI}$  the cloned sequence terminates at residue Ile223. Following that, the Leu-Asp beginning of the  $His_6$  tag at the end of  $C_{HI}$  (Leu-Asp-His-His-His-His-His) is clear in the maps. The maps also provide a hint of the first of the His residues, but the remaining ones cannot be seen with confidence.

As previously identified (Cohen *et al.*, 1996), proline residues Pro8<sub>L</sub>, Pro141<sub>L</sub>, Pro149<sub>H</sub>, Pro151<sub>H</sub> and Pro202<sub>H</sub> are all in the *cis* confirmation. Four residues in the loop joining the first two strands of  $C_{HI}$ , 128, 129, 130 and 133, are in poor density in the electron-density maps; they have been modeled primarily according to stereochemical considerations. Six residues, 22, 24, 29, 72 and 106 of  $V_L$ , and 62 of the bound lysozyme molecule, have been modeled as disordered with two side-chain rotamers, each having an occupancy of 0.5. The final model contains 619 water molecules.

### 3. Results

#### 3.1. The Fab-lysozyme interface

We define the antibody-lysozyme interface residues as those residues of the antibody and lysozyme whose van der Waals surfaces come within 3.0 Å of each other as calculated by the *MS* program suite. The total buried surface area is 1337 Å<sup>2</sup>, discounting water molecules. There are two solvent-inaccessible cavities between the two interacting surfaces that are occupied by two water molecules each. Three additional buried waters are located at other sites within the interface. An additional 63 water molecules are associated with the interface and its periphery, increasing the total buried surface area to 1933 Å<sup>2</sup>.

A significant feature in the interface is the presence of salt bridges involving Glu50<sub>H</sub> with Arg45<sub>Y</sub> and Arg68<sub>Y</sub>. The importance of these salt bridges in stabilizing the HyHEL-5-lysozyme complex has been established through isothermal titration calorimetry (Wibbenmeyer, Schuck *et al.*, 1999) and is consistent with the previously reported structure of the complex and with the complex formed by HyHEL-5 with bobwhite quail lysozyme (Chacko *et al.*, 1996).

We find 70 water molecules located near to the interface of the HyHEL-5-lysozyme complex. As noted above, seven of these waters are buried in the interface between the lysozyme and the antibody and are inaccessible to solvent. Seven others are in solvent-accessible channels that penetrate a few angstroms into the interface between the lysozyme and the Fab. The remaining 56 are on the periphery of the interface and extend the effective size of the interface beyond that of the protein-protein contact alone. There are 13 protein-protein hydrogen bonds, 11 water molecules involved in protein-water-protein hydrogen bonds, 25 water molecules positioned to provide 18 hydrogen-bond bridges of the form protein-water-water-protein, three hydrogen-bond bridges involving three water molecules each and a number of van der Waals contacts. The water molecules associated with and bridging the interface have an average temperature factor that

is slightly below the average temperature factor of the complete set of 619 waters in the structure. The interface and its vicinity also contains side-chain stacking and water molecule to aromatic ring hydrogen bonding (Fig. 1); one such hydrogen bond is part of the cross-interface hydrogen bonding.

An analysis of the interface using *CONTACSYM* shows that 19 residues from the Fab, representing all six CDR regions, are in contact with 13 lysozyme residues. When the bridging waters are included in the analysis of the interface interactions, an additional four Fab residues and two lysozyme residues become indirectly involved in the interface through the water molecules. We have added these six residues to the interface that was originally calculated in the absence of water. All potential hydrogen-bond donors and acceptors within the interface are satisfied either by direct contact across the interface or through the associated waters.

The antibody-antigen interface was also examined by evaluating its shape complementarity,  $S_c$ . Lawrence & Colman (1993) defined this measure to reflect the physical fit between the surfaces of two components of a protein assembly. As an example of the measure, the then current early model of the HyHEL-5-lysozyme complex (PDB code 2hfl) was included along with several other antibody-antigen complexes as one class of interfaces (Table 1 of Lawrence & Colman, 1993). They noted consistently lower values of  $S_c$  for antigen-antibody interfaces in comparison to  $S_c$  for protein-protein inhibitor and oligomeric interfaces. They propose that this relatively poorer interface match may arise from the need for this type of interface to adapt its fit as needed. With our later model, PDB code 3hfl, as well as our current model, we find

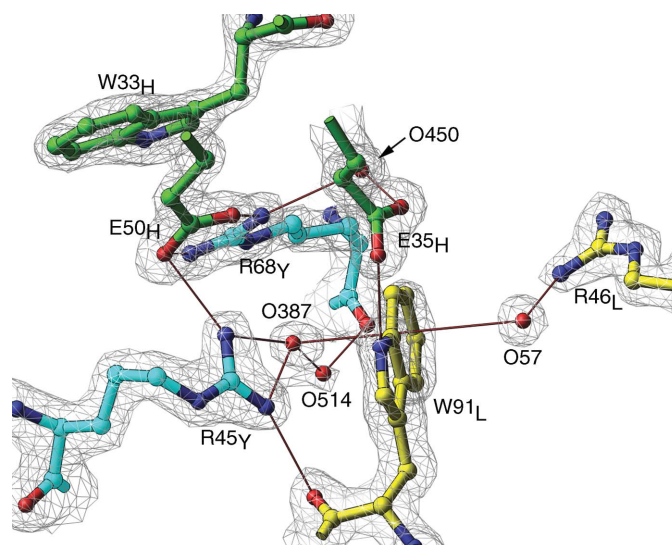


**Figure 1**  
Detailed view of the interactions between seven residues involved in the contacts between the bound lysozyme and the HyHEL-5 antibody. Two residues from lysozyme are shown with blue bonds, two residues from the antibody light chain are shown with yellow bonds and three residues from the heavy chain are shown with green bonds. Hydrogen bonding is shown with thin black bonds. The electron density from a  $2F_o - F_c$  map is contoured at  $1.8\sigma$ . The diagram was prepared with *Ribbons* v.3.12 (Carson, 1997).

that this observation may have an alternative explanation. The magnitudes of  $S_c$ , in the absence of waters, for the complex interfaces of 2hfl, 3hfl and the current model are 0.646, 0.712 and 0.719, respectively. The values for 3hfl and the current model are in the same range as most of the other models in Table 1 of Lawrence & Colman (1993), suggesting that the apparent low values for the antibody–antigen interfaces noted by Lawrence and Coleman may originate from the degree of refinement and, in some cases, the resolution of the data of the various models. The above values of  $S_c$  for the HyHEL-5–lysozyme complex were calculated omitting the waters in the model. If the 70 interface water molecules are included in the calculation,  $S_c$  increases to 0.752.

### 3.2. Other features of the interface

When all waters are removed from the current high-resolution structure, two solvent-inaccessible cavities are found within the Fab–lysozyme interface and a third between  $V_L$  and  $V_H$ . The total volume enclosed in the two cavities located in the Fab–lysozyme interface is  $108 \text{ \AA}^3$ . These two cavities contain two water molecules each. The cavity between  $V_L$  and  $V_H$  contains four waters in a volume of  $121 \text{ \AA}^3$ . In the earlier lower resolution model of this complex, 3hfl, this third cavity appeared to be joined to one of the cavities in the Fab–lysozyme interface and the water content of the cavities could not be fully defined. Three other small cavities are located within the Fab and the lysozyme and are distant from the interface.

Several interactions within the interface involve aromatic rings. A  $3.1 \text{ \AA}$  hydrogen bond is made from Wat387 to the aromatic side chain of Trp91<sub>L</sub> (Fig. 1). The vector from the center of the outer ring of the indole to Wat387 is  $7.2^\circ$  off the ring perpendicular. A second water, Wat57, is buried just below the surface of the Fab on the other side of the indole ring, making a  $3.4 \text{ \AA}$  hydrogen bond with this ring and an angle of  $4.9^\circ$  to the ring perpendicular. Both of these waters are positioned near the most optimal distance and angle in relation to the indole ring for a water molecule to aromatic ring hydrogen bond, yielding hydrogen bonds that are each approximately half the strength of conventional hydrogen bonds (Levitt & Perutz, 1988). In addition,  $N^{72}$  of Arg45 is  $2.99 \text{ \AA}$  from Wat387 and  $3.46 \text{ \AA}$  from the plane of the five-member ring of Trp91<sub>L</sub>. The side chain of Arg68<sub>Y</sub> stacks against the side chain of Trp33<sub>H</sub> with a separation of  $3.5 \text{ \AA}$ ; the planes of the Trp33<sub>H</sub> indole and the guanidinium group of Arg68<sub>Y</sub> make an angle of approximately  $7^\circ$  to each other.

## 4. Discussion

There is substantial evidence that water plays a significant role in the formation of antibody–antigen complexes (Goldbaum *et al.*, 1996). Thermodynamic studies as well as crystallography have demonstrated that the number of waters associated with the complex can be greater or less than the number associated with the isolated components. Whereas solvent molecules may be excluded in regions of the complex interface that are highly

**Table 2**

Solvation and intermolecular crystal contacts in the HyHEL-5 epitope region of lysozyme structures studied at 100 K.

PDB code	Temperature (K)	Waters	Contacts	Resolution (Å)	Space group
1dpw	100	50	18	1.64	$P4_32_12$
1dpx	100	58	19	1.65	$P4_32_12$
1gwd	100	38	17	1.77	$P4_32_12$
1h87	100	59	17	1.72	$P4_32_12$
1lz8	120	63	19	1.53	$P4_32_12$
1n4f	100	42	20	1.78	$P4_32_12$
1ps5	100	49	24	2.00	$C2$
Average		$51.3 \pm 7.5$	$19.1 \pm 1.6$		

complementary, there are often some completely buried waters as well as waters associated with the interface periphery. In order to estimate by crystallographic means the changes in bound waters upon formation of the complex, it is necessary to know the waters associated with the complex and with the two isolated components.

We have not been able to grow crystals of the uncomplexed HyHEL-5 Fab molecule and therefore cannot obtain a direct count of the number of water molecules bound at the paratope of the uncomplexed antibody molecule. Consequently, the water count must be estimated from an examination of other antibody surfaces. The structure of the D44.1 antibody (PDB code 1mlb; Braden *et al.*, 1994) seemed to be an ideal source for this information since this antibody is involved with nearly the same epitope on lysozyme as HyHEL-5 Fab. However, although the resolution of this structure is a reasonable  $2.1 \text{ \AA}$ , the number of waters in the region of the uncomplexed paratope is only 14. This appears to be too few waters in comparison with the D1.3 Fv structure (PDB code 1vfa; Bhat *et al.*, 1994), which has 29 waters on its uncomplexed paratope (Braden *et al.*, 1994). The area of the D1.3 antibody paratope is only 90% that of the D44.1 antibody paratope, but is reported to have 60% more waters associated with it. We have therefore chosen the 1vfa structure as the model with which to estimate the number of waters bound to the HyHEL-5 paratope. This uncomplexed D1.3 binds 29 water molecules in the vicinity of its lysozyme paratope and, since the area of the HyHEL-5 paratope is about 20% larger than that of D1.3, we estimate that 35 waters are located at the uncomplexed HyHEL-5 paratope.

Table 2 lists seven PDB-deposited hen egg-white lysozyme structures studied at approximately 100 K, as was the HyHEL-5 complex with lysozyme, in the resolution range  $1.5\text{--}2.0 \text{ \AA}$  [PDB codes 1dpw and 1dpx (Weiss *et al.*, 2000), 1gwd (Evans & Bricogne, 2002), 1h87 (Girard *et al.*, 2002), 1lz8 (Dauter *et al.*, 1999), 1n4f (Retailleau & Prangé, 2003) and 1ps5 (Majeed *et al.*, 2003)]. The number of waters within  $3.5 \text{ \AA}$  of the epitope ranges from 38 to 63, with an average of 51. This suggests that the minimum number of waters on the unbound epitope for HyHEL-5 of lysozyme is at least 38 and may well be somewhat closer to the average of 51.

The thermodynamic studies on the HyHEL-5 complex with lysozyme by Xavier *et al.* (1997) suggest a net gain of 6–12

water molecules upon complex formation, implying that we should find at least 79–85 waters in the complex interface. We must note, however, that our structural results on the complex, as well as the quoted results on the lysozyme structures, were obtained at liquid-nitrogen temperature, under which conditions we would expect more waters to be visible in the structure owing to the probable decrease in thermal parameters. Because the D1.3 antibody structure was determined at room temperature, we would expect an even larger number of waters on its epitope if the results were also obtained at liquid-nitrogen temperature, suggesting an even greater number of waters to be found in the interface of the complex should a net gain be observed. However, our structural results on the HyHEL-5–lysozyme complex show only 70 waters in the interface and its periphery. This is less than the conservative sum of the waters on the epitope and paratope without any gain upon complex formation. Within the limitations of the available data, therefore, we find an apparent loss of waters in the complex interface compared with the waters near the uncomplexed surfaces. While part of this discrepancy might be accounted for by the uncertainty in estimating the number of waters on the isolated HyHEL-5, the result is not immediately concordant with that of Xavier *et al.* (1997).

It should be kept in mind, however, that the measurements of Xavier *et al.* (1997) were carried out in the presence of large concentrations of osmolytes. It is possible that in the dehydrating osmolyte solution some waters which would be weakly associated with free antibody and lysozyme in pure water are absent or of lower occupancy. The osmolyte could also act to dehydrate the complex, but the waters that we observe in the crystallographic analysis would likely be relatively tightly associated and less removable. The net effect would then be to enhance the biophysically observed water uptake in comparison to the crystallographically observed waters.

In their reassessment of the D1.3–lysozyme complex, Braden *et al.* (1994) also note a loss rather than a gain in the count of bound waters, contrary to the expectation from their titration calorimetric studies of the D1.3–lysozyme association. While noting the loss of water molecules upon forming the D1.3–lysozyme complex, they also note that the shared interface waters contribute a net increase in the total number of hydrogen bonds within the interface. These water molecules also fill what would be cavities within the complex interface if the waters were not present. In the case of the HyHEL-5–lysozyme complex, several residues of the lysozyme antigen have undergone some small rearrangement in combining with the Fab and it is likely that some antibody residues would also have done so, but without a structure for the uncomplexed antibody we cannot fully evaluate these factors. We find only a few cavities in the interface, all of which are filled with waters.

There is, however, another major problem in determining the number of water molecules on molecular surfaces as observed in the crystal. The apparent number of waters bound to the uncomplexed antibodies and antigens can be influenced by hydrogen-bond or other close contacts between molecules that arise from crystal packing. Such contacts are likely to reduce the apparent number of waters at the unbound epitope

or paratope. Both the D1.3 and E8 Fabs as well as their antigens exhibit this problem.

The D1.3 Fv structure shows ten hydrogen-bonding contacts between the paratope and residues of neighboring D1.3 Fv molecules in the crystal. In the seven lysozyme structures referenced in Table 2, we find four to nine such contacts from the D1.3 epitope to neighboring lysozyme molecules in the crystal.

The complex of E8 Fab with cytochrome *c* antigen (PDB code 1wej; Mylvaganam *et al.*, 1998) appears to be in reasonable agreement with their results of isothermal titration calorimetry in comparison with the E8 Fab (PDB code 1qbl; Mylvaganam *et al.*, 1998) and the cytochrome *c* antigen (PDB code 1hrc; Bushnell *et al.*, 1990) that show a net loss of waters in the complex. A loss of nine waters from the interface is enumerated. Nevertheless, in the case of the cytochrome *c* antibody structure 1qbl, there are ten paratope hydrogen-bonding contacts with neighboring molecules in the crystal. In the case of the cytochrome *c* crystal structure 1hrc, there are four such contacts from the epitope region to neighboring protein molecules.

From these three examples, we suggest that crystallographic methods may not provide the most reliable estimate of the number of water molecules that are bound to the protein surfaces. Perhaps only methods such as isothermal titration calorimetry are appropriate for this task since such methods can evaluate the component molecules without the potential of significant intermolecular contacts. The HyHEL-5–lysozyme complex reported here, as well as the D1.3–lysozyme complex and the E8–cytochrome *c* complex, all seem to support this conclusion.

## References

- Bhat, T. N., Bently, G. A., Boulot, G., Greene, M. I., Tello, D., Dall'Aqua, W., Souchon, H., Schwarz, F. P., Mariuzza, R. A. & Poljak, R. A. (1994). *Proc. Natl Acad. Sci. USA*, **91**, 1089–1093.
- Braden, B. C., Fields, B. A. & Poljak, R. A. (1998). *J. Mol. Recognit.* **8**, 317–325.
- Braden, B. C., Souchon, H., Eiselé, J.-L., Bently, G. A., Bhat, T. N., Navaza, J. & Poljak, R. A. (1994). *J. Mol. Biol.* **243**, 767–781.
- Brünger, A. T. (1992). *X-PLOR Version 3.1. A System for X-ray Crystallography and NMR*. New Haven: Yale University Press.
- Brünger, A. T. (1997). *Methods Enzymol.* **277**, 366–396.
- Brünger, A. T., Adams, P. D., Clore, G. M., DeLano, W. L., Gros, P., Grosse-Kunstleve, R. W., Jiang, J.-S., Kuszewski, J., Nilges, N., Pannu, N. S., Read, R. J., Rice, L. M., Simonson, T. & Warren, G. L. (1998). *Acta Cryst.* **D54**, 905–921.
- Bushnell, G. W., Louie, G. V. & Brayer, G. G. (1990). *J. Mol. Biol.* **214**, 585–595.
- Carson, M. (1997). *Methods Enzymol.* **277**, 493–505.
- Chacko, S., Silverton, E., Kam-Morgan, L., Smith-Gill, S., Cohen, G. & Davies, D. (1995). *J. Mol. Biol.* **245**, 261–274.
- Chacko, S., Silverton, E. W., Smith-Gill, S. J., Davies, D. R., Shick, K. A., Xavier, K. A., Willson, R. C., Jeffrey, P. D., Chang, C. Y. Y., Sieker, L. C. & Sheriff, S. (1996). *Proteins*, **26**, 55–65.
- Cohen, G. H. (1997). *J. Appl. Cryst.* **30**, 1160–1161.
- Cohen, G. H., Sheriff, S. & Davies, D. R. (1996). *Acta Cryst.* **D52**, 315–326.
- Connolly, M. L. (1983). *J. Appl. Cryst.* **16**, 548–558.

- Dall'Aqua, W., Goldman, E. R., Lin, W., Teng, C., Tsuchiya, D., Li, H., Ysern, X., Braden, B. C., Li, Y., Smith-Gill, S. J. & Mariuzza, R. A. (1998). *Biochemistry*, **37**, 7981–7991.
- Dauter, Z., Dauter, M., de La Fortelle, E., Bricogne, G. & Sheldrick, G. M. (1999). *J. Mol. Biol.* **289**, 83–92.
- Engh, R. A. & Huber, R. (1991). *Acta Cryst.* **A47**, 392–400.
- Evans, G. & Bricogne, G. (2002). *Acta Cryst.* **D58**, 976–991.
- Fields, B. A., Goldbaum, F. A., Dall'Aqua, W., Malchiodi, E. L., Cauerhff, A., Schwarz, F. P., Ysern, X., Poljak, R. J. & Mariuzza, R. A. (1996). *Biochemistry*, **35**, 15494–15503.
- Girard, É., Chantalat, L., Vicat, J. & Kahn, R. (2002). *Acta Cryst.* **D58**, 1–9.
- Goldbaum, F. A., Schwartz, F. P., Eisenstein, E., Cauerhff, A., Maruizza, R. A. & Poljack, R. J. (1996). *J. Mol. Recognit.* **9**, 6–12.
- Jones, T. A., Zou, J. Y., Cowan S. W. & Kjeldgaard, M. (1991). *Acta Cryst.* **A47**, 110–119.
- Kabat, E. A., Wu, T. T., Reid-Miller, M., Perry, H. M. & Gottesman, K. S. (1987). *Sequences of Immunological Interest*, 4th ed. Bethesda, Maryland, USA: National Institutes of Health.
- Kondo, H., Shiroishi, M., Matsushima, M., Tsumoto, K. & Kumagai, I. (1999). *J. Biol. Chem.* **274**, 27623–27631.
- Kleywegt, G. J. & Jones, T. A. (1996). *Acta Cryst.* **D52**, 826–828.
- Lawrence, M. C. & Colman, P. M. (1993). *J. Mol. Biol.* **234**, 946–950.
- Levitt, M. & Perutz, M. F. (1988). *J. Mol. Biol.* **201**, 751–754.
- Majeed, S., Ofek, G., Belachew, A., Huang, C., Zhou, T. & Kwong, P. D. (2003). *Structure*, **11**, 1061–1070.
- Malby, R. L., Tulip, W. R., Harley, V. R., McKimm-Breschkin, J. L., Laver, W. G., Webster, R. G. & Coleman, P. M. (1994). *Structure* **2**, 733–746.
- Milner-White, E. J. & Poet, R. (1987). *Trends Biochem. Sci.* **12**, 198–192.
- Milner-White, E. J., Ross, B. M., Ismail, R., Belhaj-Mostefa, K. & Poet, R. (1988). *J. Mol. Biol.* **204**, 777–782.
- Monaco-Malbet, S., Berthet-Colominas, C., Novelli, A., Battaï, N., Piga, N., Cheynet, V., Mallet, F. & Cusak, S. (2000). *Structure*, **8**, 1069–1077.
- Mylvaganam, S. E., Paterson, Y. & Getzoff, E. D. (1998). *J. Mol. Biol.* **281**, 301–322.
- Otwinowski, Z. & Minor, W. (1997). *Methods Enzymol.* **276**, 307–326.
- Retailleau, P. & Prangé, T. (2003). *Acta Cryst.* **D59**, 887–896.
- Sheriff, S., Hendrickson, W. A. & Smith, J. L. (1987). *J. Mol. Biol.* **197**, 273–296.
- Sheriff, S., Silverton, E. W., Padlan, E. A., Cohen, G. H., Smith-Gill, S. J., Finzel, B. C. & Davies, D. R. (1987). *Proc. Natl Acad. Sci. USA*, **84**, 8075–8079.
- Tulip, W. R., Varghese, J. N., Webster, R. G., Laver, W. G. & Coleman, P. M. (1992). *J. Mol. Biol.* **227**, 149–159.
- Weiss, M. S., Palm, G. J. & Hilgenfeld, R. (2000). *Acta Cryst.* **D56**, 952–958.
- Wibbenmeyer, J. A., Schuck, P., Smith-Gill, S. J. & Willson, R. C. (1999). *J. Biol. Chem.* **274**, 26838–26842.
- Wibbenmeyer, J. A., Xavier, K. A., Smith-Gill, S. J. & Willson, R. C. (1999). *Biochem. Biophys. Acta*, **1430**, 191–202.
- Xavier, K. A., Shick, K. A., Smith-Gill, S. J. & Willson, R. C. (1997). *Biophys. J.* **73**, 2116–2125.
- Xavier, K. A. & Willson, R. C. (1998). *Biophys. J.* **74**, 2036–2045.
- Yili, Y., Urrutia, M., Smith-Gill, S. J. & Mariuzza, R. A. (2000). *Biochemistry*, **39**, 6296–6309.
- Yili, Y., Urrutia, M., Smith-Gill, S. J. & Mariuzza, R. A. (2003). *Biochemistry*, **42**, 11–22.